



Hyperbolic surface waves on anisotropic materials without hyperbolic dispersion

TAAVI REPÄN,^{1,2,*}  OSAMU TAKAYAMA,¹  AND ANDREI LAVRINENKO¹

¹*DTU Fotonik, Technical University of Denmark, Ørstedts Plads 343, DK-2800 Kongens Lyngby, Denmark*

²*Institute of Nanotechnology, Karlsruhe Institute of Technology, 76021 Karlsruhe, Germany*

*taavi.repaen@kit.edu

Abstract: We theoretically analyze directional surface electromagnetic waves supported at an interface between an isotropic medium and anisotropic metal with effective uniaxial negative permittivity. We identify two types of surface wave solutions, resulting in unique hyperbolic dispersion in the wavevector space. Such anisotropic metal can be realized by alternating dielectric and metallic layers with deep subwavelength thicknesses or metallic nanowires in dielectric host. Such systems serve as a platform for many applications in nanophotonics.

© 2020 Optical Society of America under the terms of the [OSA Open Access Publishing Agreement](#)

1. Introduction

Photonic surface waves, or simply surface waves, are propagating electromagnetic modes localized at the interface of two dissimilar media, whose electromagnetic fields decay exponentially away from the interface [1,2]. Various types of surface waves are known to date including surface plasmon polaritons supported at the interfaces with metals [3], Dyakonov surface waves at the interfaces with anisotropic dielectrics [4–10], Bloch surface waves on dielectric photonic crystals [11–13], and Tamm states on anisotropic materials [14,15]. Surface waves have been used for sensing [13], waveguiding [16], steering of signals [10,17,18]. Moreover, recently surface waves on anisotropic 2D materials [19,20] have been extensively investigated.

Hyperbolic metamaterials (HMMs) are distinguished by their extreme uniaxial anisotropy, having both negative and positive permittivity tensor components characterized by ϵ_o and ϵ_e [21–24]. Propagation of waves, bulk plasmons, in such media is characterized by hyperbolic dispersion. The unbounded nature of the hyperbolic dispersion relation corresponds to existence of modes with high spatial frequencies in a real case. These special properties lead to a wide range of applications, including far-field subwavelength imaging, engineering density of states for quantum emitters and sensing [25–27].

Propagating surface plasmons on anisotropic structures (Dyakonov plasmons) are also governed by hyperbolic-like dispersion in the plane of the interface [28,29]. In the literature so far it has been assumed that for hyperbolic surface waves (HSWs) it is required either (1) an interface between a metal and an anisotropic dielectric ($\epsilon_o > 0$ and $\epsilon_e > 0$) or (2) an interface between a HMM ($\epsilon_o \epsilon_e < 0$) and an isotropic dielectric [28]. The former has been theoretically analysed by Li *et al.* [30], but so far most of attention has been devoted to the latter case (based on HMMs) [31], with a number of experimental demonstrations [32–35].

Losses are an important concern in engineering surface-wave-based devices. While material losses affect both bulk and surface waves, for the latter case additional challenges arise from the parasitic scattering from surface structures to free space modes [36–38]. Notably, surface waves on HMM based structures have an additional source of losses apart from absorption loss [39], via scattering to high- k modes present in the HMM (high photonic density of states). Thus enabling engineering of HSWs while avoiding HMMs allows to block a significant source of scattering losses.

Here we show that HSWs can exist under general conditions which do not require a HMM—dielectric interface. We explore the interface formed by an isotropic dielectric and an anisotropic medium described by negative permittivity tensor components ($\varepsilon_o < 0$ and $\varepsilon_e < 0$). We reveal that depending on the permittivity tensor components such anisotropic interfaces support two types of HSWs, which is similar to the ones on HMM-based interfaces but avoiding drawbacks of scattering loss on HMM-based interfaces. HSWs on anisotropic interface may enable engineering of surface wave propagation.

2. Theory

We consider a planar interface ($z = 0$) between an anisotropic medium [with permittivity tensor $\hat{\varepsilon} = \text{diag}(\varepsilon_e, \varepsilon_o, \varepsilon_o)$] and cover isotropic dielectric medium ($\varepsilon_c > 0$), as illustrated in Fig. 1. Note that the anisotropic media can be either deep subwavelength metal-dielectric trenches (grating) or metal nanowires in dielectric host.

$$\mathbf{E}_{\text{TE}} = E_0^{(\text{TE})} \exp(i\mathbf{k}_c \mathbf{r}) (k_y \hat{x} - k_x \hat{y}) / k_c, \quad (1)$$

$$\mathbf{H}_{\text{TM}} = H_0^{(\text{TM})} \exp(i\mathbf{k}_c \mathbf{r}) (k_y \hat{x} - k_x \hat{y}) / k_c, \quad (2)$$

while in the anisotropic media there are ordinary and extraordinary modes

$$\mathbf{E}_o = N_o \exp(i\mathbf{k}_o \mathbf{r}) (k_z^o \hat{y} - k_y \hat{z}), \quad (3)$$

$$\mathbf{E}_e = N_e \exp(i\mathbf{k}_e \mathbf{r}) \left[- (k_0^2 \varepsilon_o - k_x^2) \hat{x} + k_x k_y \hat{y} + k_z^e k_x \hat{z} \right], \quad (4)$$

where N_o and N_e are normalization coefficients [40]. The wavevectors are defined as $\mathbf{k}_i = k_x \hat{x} + k_y \hat{y} + k_z^i \hat{z}$ with $i = c, o, e$. They have to satisfy dispersion relations [41,42]

$$k_x^2 + k_y^2 + (k_z^c)^2 = \varepsilon_c k_0^2, \quad (5)$$

$$k_x^2 + k_y^2 + (k_z^o)^2 = \varepsilon_o k_0^2, \quad (6)$$

$$k_x^2 / \varepsilon_o + k_y^2 / \varepsilon_e + (k_z^e)^2 / \varepsilon_e = k_0^2. \quad (7)$$

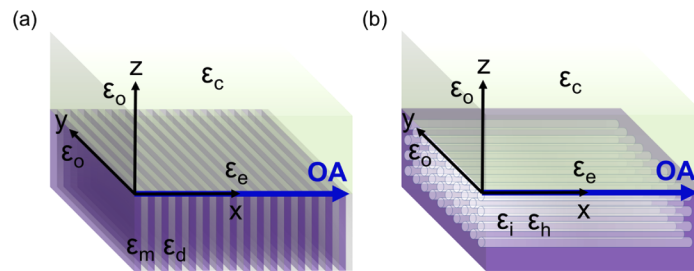


Fig. 1. Geometry of the anisotropic interfaces with optical axis (OA) of the uniaxial medium aligned along the x -axis with effective ordinary and extraordinary permittivities, ε_o and ε_e , respectively and isotropic cover layer with permittivity ε_c . (a) Metal-dielectric multilayer with permittivity of metal and dielectric layers ε_m and ε_d , respectively. (b) metal nanowire in dielectric host with permittivity of metal nanowire and dielectric host, ε_i and ε_h , respectively.

First we establish the limiting cases of propagation along either the x or y direction. Enforcing electromagnetic interface conditions and requiring fields to be evanescent on both sides of the

interface leads to solutions with the propagation constants (for the ordinary and the extraordinary case, respectively)

$$\beta_o = \sqrt{\frac{\varepsilon_o \varepsilon_c}{\varepsilon_o + \varepsilon_c}} k_0, \quad (8)$$

$$\beta_e = \sqrt{\frac{\varepsilon_e \varepsilon_c - \varepsilon_c^2}{\varepsilon_e - \varepsilon_c^2 / \varepsilon_o}} k_0. \quad (9)$$

From these equations we can identify the condition that must be fulfilled for the interface to support a propagating mode along the y direction

$$\varepsilon_o + \varepsilon_c < 0 \quad (10)$$

and the similar condition for the mode propagating along the x axis

$$\varepsilon_e - \varepsilon_c^2 / \varepsilon_o < 0. \quad (11)$$

In deriving condition (11), we assume that $\varepsilon_e < \varepsilon_c$, because for the other case $\beta_e < \sqrt{\varepsilon_c} k_0$ and thus the solution would not represent a surface wave. If the material parameters are such that only one of conditions (10) and (11) is fulfilled, then the anisotropic interface exhibits a transition between propagating and evanescent surface waves, leading to hyperbolic-like dispersion of surface waves. Here, we define two types of HSWs as HSW-1 that satisfies condition (10) and possesses hyperbolic dispersion in wavevector space (k -space) around y -axis perpendicular to the optical axis (OA, x -axis) while HSW-2 satisfies condition (11) and has hyperbolic dispersion in k -space axis is around the optical axis (x -axis). Note that these HSWs have hyperbolic dispersion in $k_{x,y}$ space, which distinguishes HMMs with hyperbolic dispersion of bulk plasmons in $k_{x,y,z}$ space.

In Fig. 2(a) we map the conditions of ε_o , ε_e , and ε_c , specifying two different regimes for HSWs and classify these regimes with HSW-1 and HSW-2. Note that HSW-1 also includes surface waves on type-II HMM regime ($\varepsilon_o < 0$ and $\varepsilon_e > 0$) and we point out that earlier works have considered subset of HSW-1 by limiting discussion to an interface between a HMM and dielectric [28]. We emphasize that an anisotropic plasmonic metamaterial ($\varepsilon_o < 0$ and $\varepsilon_e < 0$) is sufficient to support HSWs and we focus on this case as the novelty of this article, such that avoiding HMMs removes the problem of unwanted scattering into the high- k modes.

Anisotropic metals and properties required for HSWs can be realized by periodic metamaterial structures where the period is significantly smaller than the wavelength. In such cases the structure can be approximated as a homogeneous anisotropic medium. From the fabrication standpoint the most straightforward structures exhibiting surface anisotropy are metal-dielectric trenches as illustrated in Fig. 1(a) [34]. The effective medium theory [43–45] for the trench structures (metal-dielectric multilayers) gives the effective material parameters as

$$\varepsilon_o = f_m \varepsilon_m + (1 - f_m) \varepsilon_d, \quad (12)$$

$$\varepsilon_e^{-1} = f_m \varepsilon_m^{-1} + (1 - f_m) \varepsilon_d^{-1}, \quad (13)$$

where f_m is the volume filling fraction of metallic component with ε_m , permittivity of dielectric layers, ε_d . Assuming alternating Ag/TiO₂ layers with $\varepsilon_d = 2.3^2 - 2.4^2$ for atomic layer deposited TiO₂ film measured by ellipsometer and ε_m of Ag from Ref [46], the multilayer structure behave as highly anisotropic material with different combination of effective permittivities. The structure behaves as anisotropic metal ($\varepsilon_o < 0$ and $\varepsilon_e < 0$) for certain volume fraction of metal and by checking the resulting effective medium parameters against conditions for HSWs [conditions (10) and (11)], they support HSW-2 for $\lambda = 415 \text{ nm} - 495 \text{ nm}$ as plotted in Fig. 2(b). Note that

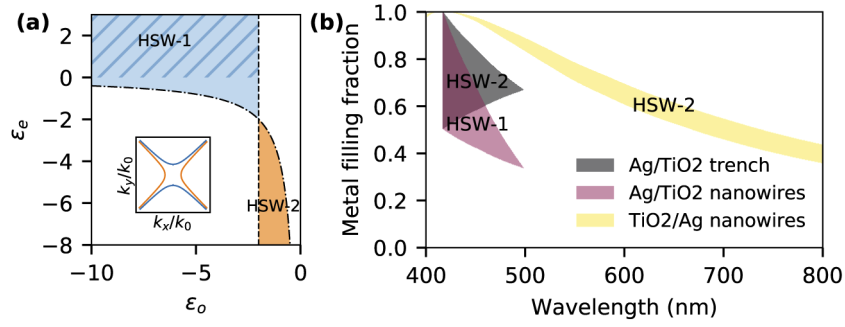


Fig. 2. (a) Conditions (10) (dash-dotted line) and (11) (dashed line) indicating two different types of hyperbolic surface waves. Striped region indicates the type-II HMM regime ($\epsilon_o < 0 < \epsilon_e$) inside the HSW-1 area. Inset shows typical spatial dispersion in $k_{x,y}$ space for HSW-1 and HSW-2 indicated by the blue and orange lines, respectively. Note that $\epsilon_c = 2$, corresponds to the vertical dashed line and dot-dashed line corresponds to $\epsilon_e = \epsilon_c^2/\epsilon_o$. (b) Operating wavelengths and metal filling fractions of Ag/TiO₂ trench, Ag/TiO₂ nanowire, and TiO₂/Ag nanowire systems, yielding effective medium parameters suitable for HSWs ($\epsilon_o < 0$ and $\epsilon_e < 0$) and types of HSWs, calculated without the loss of materials, imaginary part of permittivities. HSW-1 exhibits hyperbolic dispersion around y-axis perpendicular to the optical axis (OA, x-axis) while HSW-2 has that around the optical axis. Note that Ag/TiO₂ nanowires are Ag nanowires in TiO₂ host and TiO₂/Ag nanowires are TiO₂ nanowires in Ag host. The lower wavelength limit at 415 nm for both HSW-1 and -2 is where $\epsilon_m + \epsilon_d = 0$. The upper wavelength limit of HSW-1 at 495 nm is at the crossing between $\epsilon_e - \epsilon_c^2/\epsilon_o = 0$ (upper boundary) and $\epsilon_e = 0$ (lower boundary), and that of HSW-2 is at the crossing between $\epsilon_o + \epsilon_c = 0$ and $1/\epsilon_e = 0$, respectively.

trench structures only allow obtaining HSW-2, but for achieving HSW-1 they will not suffice, as $\epsilon_o > \epsilon_e$ always holds whenever $\epsilon_e < 0$.

Instead, nanowire structures could be employed with effective anisotropic parameters calculated by the following equations

$$\epsilon_o = \epsilon_h \frac{(1 + f_i) \epsilon_i + (1 - f_i) \epsilon_h}{(1 + f_i) \epsilon_h + (1 - f_i) \epsilon_i}, \quad (14)$$

$$\epsilon_e = f \epsilon_i + (1 - f) \epsilon_h, \quad (15)$$

where f_i is the volume filling fraction of the metallic inclusions (permittivity ϵ_i) in the host dielectric medium with permittivity ϵ_h , as illustrated in Fig. 1(b) [47]. It is possible to fulfill conditions for HSWs by aligning nanowires parallel to the interface, so that the optical axis of the effective medium is parallel to the interface. We consider Ag nanowires in the TiO₂ host and show the domain where HSW-1 are supported for $\lambda = 415 \text{ nm} - 495 \text{ nm}$ [the red shaded region in Fig. 2(b)]. To fulfill HSW conditions at longer wavelengths TiO₂ nanowires in the Ag host could also be considered.

Exact dispersion relation of surface waves on an anisotropic interface has been derived by Dyakonov [4]

$$(k_y + k_y^e) (k_y + k_y^o) (\epsilon_c k_y^o + \epsilon_o k_y^e) = -(\epsilon_e - \epsilon_c) (\epsilon_c - \epsilon_o) k_y^o k_0^2, \quad (16)$$

where k_y , k_y^o , and k_y^e satisfy

$$N^2 - k_y^2 = \epsilon_c \quad (17)$$

$$\frac{N^2 \sin^2 \theta - (k_y^e)^2}{\epsilon_e} + \frac{N^2 \cos^2 \theta}{\epsilon_o} = 1 \quad (18)$$

$$N^2 - (k_y^o)^2 = \varepsilon_o. \tag{19}$$

Here, N is the normalized wavevector and θ is an angle from the optical axis in x-y plane. Although Eq. (16) was used in the context of anisotropic dielectric media in elliptic regime ($\varepsilon_o > 0$ and $\varepsilon_e > 0$) [4–6,9,10] and HMM ($\varepsilon_o < 0$ and $\varepsilon_e > 0$) – dielectric interfaces [28,31,34,35,48–50], this equation also covers HSW-1 and HSW-2 on anisotropic metals ($\varepsilon_o < 0$ and $\varepsilon_e < 0$) as introduced above. Equation (16) is in the implicit form, so obtaining dispersion of the HSWs (allowed k_x and k_y) is not straightforward. However, after plotting the solution for Eq. (16) (Fig. 3) we see that it resembles hyperbolic dispersion of bulk modes in HMM given by

$$\frac{k_x^2}{\varepsilon_y} + \frac{k_y^2}{\varepsilon_x} = k_0^2, \tag{20}$$

where $\varepsilon_x, \varepsilon_y$ are components of a corresponding HMM permittivity tensor. In contrast to Eq. (16), this explicit equation is easy to solve for k_x and k_y , thus giving a useful approximation for HSW behavior. To show approximate equivalence we consider two limiting cases: $k_x = 0$ and $k_x \rightarrow \infty$. In case of Eq. (20) we obtain

$$k_y|_{k_x=0} = \sqrt{\varepsilon_x} k_0, \tag{21}$$

$$\lim_{k_x \rightarrow \infty} k_y = k_x \sqrt{-\frac{\varepsilon_x}{\varepsilon_y}}. \tag{22}$$

Similarly, with Eq. (16) we get

$$k_y|_{k_x=0} = \sqrt{\frac{\varepsilon_c \varepsilon_o}{\varepsilon_c + \varepsilon_o}} k_0, \tag{23}$$

$$\lim_{k_x \rightarrow \infty} k_y = \sqrt{-\frac{\varepsilon_c^2 - \varepsilon_e \varepsilon_o}{\varepsilon_c^2 - \varepsilon_o^2}} k_x. \tag{24}$$

Now we can establish equivalence between the exact HSW dispersion Eq. (16) and the (approximate) hyperbolic dispersion Eq. (20). Equating Eq. (21) with Eq. (24) yields solution for equivalent parameters

$$\varepsilon_x = \frac{\varepsilon_d \varepsilon_o}{\varepsilon_d + \varepsilon_o}, \tag{25}$$

$$\varepsilon_y = \frac{(\varepsilon_d - \varepsilon_o) \varepsilon_d \varepsilon_o}{\varepsilon_d^2 - \varepsilon_e \varepsilon_o}. \tag{26}$$

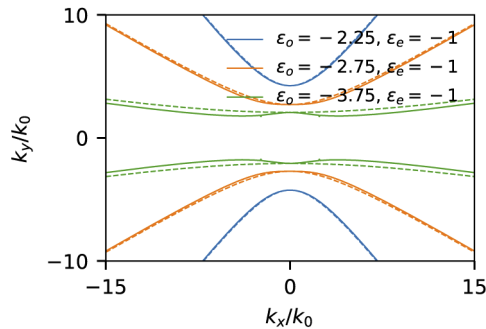


Fig. 3. Spatial dispersion of HSW-1 with various permittivity parameters according to the exact Dyakonov equation Eq. (16) and hyperbolic approximation Eq. (20), shown with solid and dashed lines, respectively.

3. Result and discussion

Knowing that type-I ($\epsilon_o > 0$ and $\epsilon_e < 0$) and type-II ($\epsilon_o < 0$ and $\epsilon_e > 0$) HMMs [25] exhibit opposite phase propagation properties [51], we might expect the same for HSW-1 and HSW-2. This can be seen in Fig. 4, where fields and also phase propagation directions for the two types of HSWs are plotted. Comparing HSW-1 [Fig. 4(a)] and HSW-2 [Fig. 4(b)] indicates that phase propagation is flipped with respect to each other in the two cases. Considering propagation along the y-direction, the phase propagation is reversed for HSW-2. Backwards phase propagation has previously been reported for surface waves as well [29], although there only HMM-based HSWs were considered (allowing for only HSW-1) and thus magnetic properties were required for backwards phase propagation. In general, for HSW-1 on non-magnetic media phase propagation is always positive [29,48].

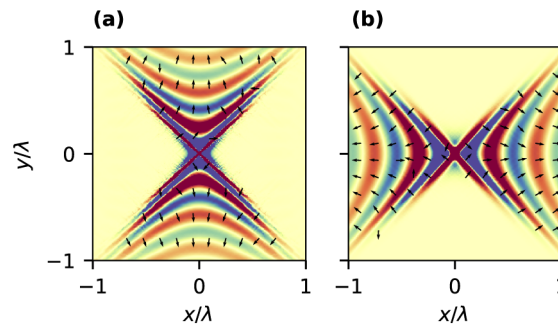


Fig. 4. Electric fields of a dipole source placed in the origin. The dipole is oriented perpendicular to the interface. A (a) HSW-1 and (b) HSW-2 are seen with $\epsilon_o = -2.48 + 0.05i$, $\epsilon_e = -0.75 + 0.05i$ and $\epsilon_o = -1 + 0.05i$, $\epsilon_e = -7 + 0.05i$, respectively. For both cases $\epsilon_c = 2$ is used. Arrows indicate direction of phase propagation.

Backwards phase propagation of HSWs can arise, because the Poynting vector can be opposite in the metal and dielectric layers due to the electromagnetic interface conditions. Thus the total energy flux $\int_{-\infty}^{\infty} P_y dz$ (integrated Poynting vector) can be either parallel or antiparallel to the phase velocity. For isotropic case it is easy to demonstrate that the bigger part of the energy is contained in the dielectric and so the integrated Poynting vector coincides with the phase propagation direction. To show that this is not always the case for anisotropic media, we assume negligible contribution from TE mode in the dielectric to reach an approximate condition for backwards propagating HSWs (in the large k_x limit)

$$\frac{\epsilon_c}{\epsilon_o} - \frac{\epsilon_o}{\epsilon_c} < 0. \quad (27)$$

Comparing this against Fig. 2(a) it is evident that HSW-1 and -2 are distinguished by phase propagation direction: HSW-1 (HSW-2) have always forwards (backwards) phase propagation, as seen in Fig. 4. Note that here we are interested in phase propagation in y direction, which is reversed and negative.

4. Conclusion

In conclusion, we show that HSWs exist for more general conditions and are not limited to the interface between an HMM and dielectric. We also show that there are two kinds of HSWs, differentiated by the phase propagation direction. Importantly the HMM–dielectric interface case only allows for HSW-1, so the general case allows for more flexibility in engineering the surface wave propagation, allowing to facilitate other designs or fabrication constraints. These surface

waves are directional, and their propagation directions are sensitive to permittivities of the media at the interface. Hence, their propagation direction can be effectively controlled by changing a wavelength or material parameters for various nanophotonics applications from sensing to manipulation of light at the nanoscale.

Funding

Det Frie Forskningsråd (8022-00387B); Sihtasutus Archimedes (Kristjan Jaak scholarship); Villum Fonden (11116).

Disclosures

The authors declare no conflicts of interest.

References

1. J. Polo and A. Lakhtakia, "Surface electromagnetic waves: A review," *Laser Photonics Rev.* **5**(2), 234–246 (2011).
2. O. Takayama, A. A. Bogdanov, and A. V. Lavrinenko, "Photonic surface waves on metamaterial interfaces," *J. Phys.: Condens. Matter* **29**(46), 463001 (2017).
3. W. L. Barnes, A. Dereux, and T. W. Ebbesen, "Surface plasmon subwavelength optics," *Nature* **424**(6950), 824–830 (2003).
4. M. Dyakonov, *Sov. Phys. JETP* **67**, 714 (1988).
5. O. Takayama, L.-C. Crasovan, S. K. Johansen, D. Mihalache, D. Artigas, and L. Torner, "Dyakonov surface waves: A review," *Electromagnetics* **28**(3), 126–145 (2008).
6. O. Takayama, L. Crasovan, D. Artigas, and L. Torner, "Observation of dyakonov surface waves," *Phys. Rev. Lett.* **102**(4), 043903 (2009).
7. O. Takayama, A. Y. Nikitin, L. Martín-Moreno, L. Torner, and D. Artigas, "Dyakonov surface wave resonant transmission," *Opt. Express* **19**(7), 6339–6347 (2011).
8. O. Takayama, D. Artigas, and L. Torner, "Coupling plasmons and dyakonons," *Opt. Lett.* **37**(11), 1983–1985 (2012).
9. O. Takayama, D. Artigas, and L. Torner, "Practical dyakonons," *Opt. Lett.* **37**(20), 4311–4313 (2012).
10. O. Takayama, D. Artigas, and L. Torner, "Lossless directional guiding of light in dielectric nanosheets using dyakonov surface waves," *Nat. Nanotechnol.* **9**(6), 419–424 (2014).
11. M. Liscidini and J. E. Sipe, "Analysis of Bloch-surface-wave assisted diffraction-based biosensors," *J. Opt. Soc. Am. B* **26**(2), 279–289 (2009).
12. L. Yu, E. Barakat, T. Sfez, L. Hvozdar, J. D. Francesco, and H. P. Herzig, "Manipulating bloch surface waves in 2d: a platform concept-based flat lens," *Light: Sci. Appl.* **3**(1), e124 (2014).
13. A. Sinibaldi, N. Danz, E. Descrovi, P. Munzert, U. Schulz, F. Sonntag, L. Dominici, and F. Michelotti, "Direct comparison of the performance of bloch surface wave and surface plasmon polariton sensors," *Sens. Actuators, B* **174**, 292–298 (2012).
14. D. P. Pulsifer, M. Faryad, and A. Lakhtakia, "Observation of the Dyakonov-Tamm wave," *Phys. Rev. Lett.* **111**(24), 243902 (2013).
15. I. V. Timofeev and S. Y. Vetrov, "Chiral optical Tamm states at the boundary of the medium with helical symmetry of the dielectric tensor," *JETP Lett.* **104**(6), 380–383 (2016).
16. Z. Han and S. I. Bozhevolnyi, "Radiation guiding with surface plasmon polaritons," *Rep. Prog. Phys.* **76**(1), 016402 (2013).
17. P. V. Kapitanova, P. Ginzburg, F. J. Rodríguez-Fortuño, D. S. Filonov, P. M. Voroshilov, P. Belov, A. N. Poddubny, Y. S. Kivshar, G. Wurtz, and A. V. Zayats, "Photonic spin Hall effect in hyperbolic metamaterials for polarization-controlled routing of subwavelength modes," *Nat. Commun.* **5**(1), 3226 (2014).
18. A. A. High, R. C. Devlin, A. Dibos, M. Polking, D. S. Wild, J. Percel, N. P. de Leon, M. D. Lukin, and H. Park, "Visible-frequency hyperbolic metasurface," *Nature* **522**(7555), 192–196 (2015).
19. P. Li, I. Dolado, F. J. Alfaro-Mozaz, F. Casanova, L. E. Hueso, S. Liu, J. H. Edgar, A. Y. Nikitin, S. Vélez, and R. Hillenbrand, "Infrared hyperbolic metasurface based on nanostructured van der waals materials," *Science* **359**(6378), 892–896 (2018).
20. W. Ma, P. Alonso-González, S. Li, A. Y. Nikitin, J. Yuan, J. Martín-Sánchez, J. Taboada-Gutiérrez, I. Amenabar, P. Li, S. Vélez, C. Tollan, Z. Dai, Y. Zhang, S. Sriram, K. Kalantar-Zadeh, S.-T. Lee, R. Hillenbrand, and Q. Bao, "In-plane anisotropic and ultra-low-loss polaritons in a natural van der waals crystal," *Nature* **562**(7728), 557–562 (2018).
21. D. R. Smith and D. Schurig, "Electromagnetic Wave Propagation in Media with Indefinite Permittivity and Permeability Tensors," *Phys. Rev. Lett.* **90**(7), 077405 (2003).
22. H. N. S. Krishnamoorthy, Z. Jacob, E. Narimanov, I. Kretzschmar, and V. M. Menon, "Topological transitions in metamaterials," *Science* **336**(6078), 205–209 (2012).

23. V. P. Drachev, V. A. Podolskiy, and A. V. Kildishev, "Hyperbolic metamaterials: new physics behind a classical problem," *Opt. Express* **21**(12), 15048–15064 (2013).
24. A. Poddubny, I. Iorsh, P. Belov, and Y. Kivshar, "Hyperbolic metamaterials," *Nat. Photonics* **7**(12), 948–957 (2013).
25. O. Takayama and A. V. Lavrinenko, "Optics with hyperbolic materials [Invited]," *J. Opt. Soc. Am. B* **36**(8), F38–F48 (2019).
26. P. Shekhar, J. Atkinson, and Z. Jacob, "Hyperbolic metamaterials: fundamentals and applications," *Nano Convergence* **1**(1), 14 (2014).
27. C. L. Cortes, W. Newman, S. Molesky, and Z. Jacob, "Quantum nanophotonics using hyperbolic metamaterials," *J. Opt.* **14**(6), 063001 (2012).
28. Z. Jacob and E. E. Narimanov, "Optical hyperspace for plasmons: Dyakonov states in metamaterials," *Appl. Phys. Lett.* **93**(22), 221109 (2008).
29. W. Yan, L. Shen, L. Ran, and J. A. Kong, "Surface modes at the interfaces between isotropic media and indefinite media," *J. Opt. Soc. Am. B* **24**(2), 530–535 (2007).
30. R. Li, C. Cheng, F.-F. Ren, J. Chen, Y.-X. Fan, J. Ding, and H.-T. Wang, "Hybridized surface plasmon polaritons at an interface between a metal and a uniaxial crystal," *Appl. Phys. Lett.* **92**(14), 141115 (2008).
31. A. V. Kildishev, A. Boltasseva, and V. M. Shalaev, "Planar photonics with metasurfaces," *Science* **339**(6125), 1232009 (2013).
32. A. A. High, R. C. Devlin, A. Dibos, M. Polking, D. S. Wild, J. Perczel, N. P. De Leon, M. D. Lukin, and H. Park, "Visible-frequency hyperbolic metasurface," *Nature* **522**(7555), 192–196 (2015).
33. A. Samusev, I. Mukhin, R. Malureanu, O. Takayama, D. V. Permyakov, I. S. Sinev, D. Baranov, O. Yermakov, I. V. Iorsh, A. A. Bogdanov, and A. V. Lavrinenko, "Polarization-resolved characterization of plasmon waves supported by an anisotropic metasurface," *Opt. Express* **25**(26), 32631–32640 (2017).
34. O. Takayama, E. Shkondin, A. Bogdanov, M. E. Aryaee Pahah, K. Golenitskii, P. A. Dmitriev, T. Repän, R. Malreanu, P. Belov, F. Jensen, and A. V. Lavrinenko, "Midinfrared surface waves on a high aspect ratio nanotrench platform," *ACS Photonics* **4**(11), 2899–2907 (2017).
35. O. Takayama, P. Dmitriev, E. Shkondin, O. Yermakov, M. E. A. Panah, K. Golenitskii, F. Jensen, A. Bogdanov, and A. V. Lavrinenko, "Experimental Observation of Dyakonov Plasmons," *Semiconductors* **52**(4), 442–446 (2018).
36. J. Elser and V. A. Podolskiy, "Scattering-free plasmonic optics with anisotropic metamaterials," *Phys. Rev. Lett.* **100**(6), 066402 (2008).
37. R. F. Oulton, D. F. Pile, Y. Liu, and X. Zhang, "Scattering of surface plasmon polaritons at abrupt surface interfaces: Implications for nanoscale cavities," *Phys. Rev. B* **76**(3), 035408 (2007).
38. E. A. Bezus, L. L. Doskolovich, and N. L. Kazanskiy, "Scattering suppression in plasmonic optics using a simple two-layer dielectric structure," *Appl. Phys. Lett.* **98**(22), 221108 (2011).
39. S. Campione, T. S. Luk, S. Liu, and M. B. Sinclair, "Realizing high-quality, ultralarge momentum states and ultrafast topological transitions using semiconductor hyperbolic metamaterials," *J. Opt. Soc. Am. B* **32**(9), 1809–1815 (2015).
40. J. Lekner, "Reflection and refraction by uniaxial crystals," *J. Phys.: Condens. Matter* **3**(32), 6121–6133 (1991).
41. O. Kidwai, S. V. Zhukovsky, and J. E. Sipe, "Dipole radiation near hyperbolic metamaterials: Applicability of effective medium approximation," *Opt. Lett.* **36**(13), 2530–2532 (2011).
42. C. Guclu, S. Campione, and F. Capolino, "Hyperbolic metamaterial as super absorber for scattered fields generated at its surface," *Phys. Rev. B* **86**(20), 205130 (2012).
43. S. Rytov, "Electromagnetic properties of a finely stratified medium," *Soviet Physics JEPT* **2**, 466–475 (1956).
44. V. Agranovich, "Dielectric permeability and influence of external fields on optical properties of superlattices," *Solid State Commun.* **78**(8), 747–750 (1991).
45. L. Ferrari, C. Wu, D. Lepage, X. Zhang, and Z. Liu, "Hyperbolic metamaterials and their applications," *Prog. Quantum Electron.* **40**, 1–40 (2015).
46. P. B. Johnson and R. W. Christy, "Optical constants of the noble metals," *Phys. Rev. B* **6**(12), 4370–4379 (1972).
47. B. M. Wells, A. V. Zayats, and V. A. Podolskiy, "Nonlocal optics of plasmonic nanowire metamaterials," *Phys. Rev. B* **89**(3), 035111 (2014).
48. E. Cojocaru, "Comparative analysis of Dyakonov hybrid surface waves at dielectric–elliptic and dielectric–hyperbolic media interfaces," *J. Opt. Soc. Am. B* **31**(11), 2558–2564 (2014).
49. C. J. Zapata-Rodríguez, J. J. Miret, S. Vuković, and M. R. Belić, "Engineered surface waves in hyperbolic metamaterials," *Opt. Express* **21**(16), 19113–19127 (2013).
50. J. J. Miret, J. A. Sorní, M. Naserpour, A. G. Ardakani, and C. J. Zapata-Rodríguez, "Nonlocal dispersion anomalies of dyakonov-like surface waves at hyperbolic media interfaces," *Photonics Nanostructures - Fundamentals Appl.* **18**, 16–22 (2016).
51. T. Repän, A. Novitsky, M. Willatzen, and A. V. Lavrinenko, "Pseudocanalization regime for magnetic dark-field hyperlenses," *Phys. Rev. B* **96**(19), 195166 (2017).